Rept.

NASA CR 52615

t: GEOMAGNETIC CONTROL OF THE ELECTRON DENSITY IN THE F REGION OF THE IONOSPHERE[1]

~~X 64 10595~~ *

N65-88987

Code 2A

27p

6021307 NASA

R. A. Goldberg[2],
Goddard Space Flight Center, NASA
Greenbelt, Maryland
md.

P. C. Kendall, and
Department of Applied Mathematics
University of Sheffield U.
Sheffield, England

(NASA Wash., D.C.)

double code
8003006

6021000 E. R. Schmerling[3]
NASA Headquarters
Washington, D. C.

[1963] 27p refs Submitted for publication

[1]This research was sponsored in part by Geophysics Research Directorate, AFCRL, OAR of the Air Research and Development Command, USAF, monitored by the European Office of the Air Research and Development Command under Grant ~~No.~~ AF - EOAR - 61-41; and in part by the National Science Foundation under NSF-G-22040, and in part by NASA.

[2]National Academy of Sciences-National Research Council Post-doctoral Resident Research Associate.

[3]On leave from the Ionosphere Research Laboratory, Pennsylvania State University.

10595

Abstract. The solution of a problem recently treated by Goldberg and Schmerling [1963] is written in simple closed form. The problem concerns a possible explanation of the geomagnetic anomaly in terms of diffusion along the magnetic lines of force for a special model of the F2 layer at the magnetic equator. At great height the results obtained are roughly in agreement with observations made by the Alouette (S-27) satellite on 3 October 1962. The theoretical electron density at fixed height is given as a function of magnetic latitude for a wide range of expected conditions at various phases of the solar cycle. Curves showing the latitude variation of $[\partial (\log N)/\partial r]^{-1}$ at great height are also given. The results are discussed. AUTHOR

UNCL.

Introduction

Recently Kendall [1962, 1963] and Rishbeth, Lyon and Peart [1963] have computed electron densities in the F2 region for specific models. These investigations were made under the three chief assumptions that:

(1) the ionization only moves along the magnetic lines of force of the geomagnetic dipole.

(2) production and loss are specified, the production being according to the well known Chapman law [1931], and the loss coefficient varying exponentially with height [Ratcliffe, Schmerling, Setty and Thomas, 1956].

(3) there is no electrodynamic drift across the magnetic lines of force.

With these assumptions, and general boundary conditions, an insignificant trough of electron density is found as the magnetic dipole equator is approached.

On the other hand, Goldberg and Schmerling [1963], working with essentially the same differential equation, have considered electron density distributions with a given height profile at the dipole equator as a boundary condition. They have reached the conclusion that an appreciable equatorial trough can be maintained in the electron density N at fixed height. This paper will subsequently be referred to as GS.

Further work has now resulted in the closed form analytic solution of the problem treated in GS. This has brought out a number of new points and corrected others. The solution exhibits many features which are found in the data obtained by the Alouette (S-27) Satellite Topside Sounder. Reasonable agreement is obtained with these observations, (taken above the F2 peak), from the magnetic equator up to mid-latitudes. Other physical effects then appear to take over which have not been included in the theory.

The results obtained in GS are corrected in the sense that the equatorial through in the peak electron density, N_{max}, is now found to extend as far as the poles. It may be shown that diffusive equilibrium alone cannot reproduce the entire geomagnetic anomaly correctly. That is, no distribution in diffusive equilibrium has a minimum value of N_{max} at the dipole equator with maximum values on either side of the dipole equator.

General Discussion

In GS a power series was developed which relates the electron density, $N = N\ (r, \alpha)$, at arbitrary dipole latitude, α , to the electron density over the dipole equator ($\alpha = 0$). The vertical electron density distribution $N\ (r, 0)$, at the equator, considered as a function of the radial distance, r, from the earth's center, was taken as the boundary condition. This approach avoids the choice of any particular variation of electron production rate as a function of altitude, and leaves open the question of the mechanism which might maintain such a distribution. It was further assumed that the diffusive motion of electrons follows the lines of magnetic force, and that the distribution is in equilibrium ($\partial N/\partial t = 0$). In the initial development of the equations, neither diffusive equilibrium nor photoequilibrium was assumed. The series solution obtained in GS is, thus, quite general, although calculations were made only for the case where a term, C_3, containing the difference between production and loss, could be neglected in comparison with the other terms. This approximation improves with increasing altitude above the F2 electron peak since C_3 decreases exponentially with height, and does not imply photoequilibrium. The results obtained in GS may be derived by setting $\mathfrak{D}(N) = 0$ where $\mathfrak{D}$ is the diffusion operator defined, for example, by Kendall [1962]. This is believed to hold to a high degree of approximation at great heights in the F2 region, not because the diffusive velocity actually vanishes there, but because any significant departure from the equation $\mathfrak{D}(N) = 0$ immediately gives rise to a large diffusive flux of electrons which restores the situation. (The coefficient of diffusion increases exponentially with height, and is large at great height). This situation, known as diffusive equilibrium, is thought to prevail above the F2 electron peak.

At low altitudes, well below the F2 electron peak, production and loss are nearly equal, making $\nabla \cdot N\vec{V}$ again small. Here, however, $\mathcal{D}\,(N) \neq 0$ because the coefficient of diffusion has become small. This situation is known as photoequilibrium. The lowest altitude at which the condition $\mathcal{D}\,(N) = 0$ produces valid results is not easily derived. The peak electron density is probably produced as a balance between production, diffusion and loss. If this is so, the condition $\mathcal{D}\,(N) = 0$ would apply well above the peak.

The Solution of $\mathcal{D}\,(N) = 0$ In Closed Form

The equation for a dipole line of force may be written

$$r = r_o \cos^2 \alpha \tag{1}$$

where r is the radial distance from the center of the earth, and α is the magnetic latitude.

Assuming diffusion equilibrium along a line of force, the electron density along any particular field line may be written, after Goldberg and Schmerling [1962]

$$N\,(r, \alpha) = N\,(r_o, 0) \exp\left(\frac{r_o \sin^2 \alpha}{2H_2}\right) \tag{2}$$

where H_2 is the scale height of the ionizable constituent. Substituting from equation (1) gives

$$N\ (r,\ \alpha)\ =\ N\ (r\ \sec^2\alpha,\ 0)\ \exp\left(\frac{r\ \tan^2\alpha}{2H_2}\right). \tag{3}$$

The special equatorial model used in GS is given by

$$N\ (r,\ 0)\ =\ N\ (r_{mo},\ 0)\ \exp\tfrac{1}{2}\left[1 - k\ (r - r_{mo}) - e^{-k(r - r_{mo})}\right]. \tag{4}$$

This is an equatorial Chapman distribution with a maximum at r_{mo} and "scale height" k^{-1}. The height of the maximum at other latitudes is denoted by r_m. Using equations (3) and (4) gives

$$\begin{aligned} N\ (r,\ \alpha)\ =\ N\ (r_{mo},\ 0)\ \exp\tfrac{1}{2}\Big[1 + kr_{mo} - \left(k\ \sec^2\alpha - \frac{\tan^2\alpha}{H_2}\right) r \\ - e^{kr_{mo} - kr\ \sec^2\alpha}\Big]\ . \end{aligned} \tag{5}$$

Typical values of k and r are $k = 0.01\ \text{km}^{-1}$, $r = 6850$ km. Thus,

$$kr\ \gg\ 1 \tag{6}$$

It is also convenient to use the notation

$$F\ =\ \exp\left[-k\ (r - r_{mo})\right]$$

Using the inequality (6) to neglect small quantities consistently, we find that the power series expansion of (5) in powers of α^2 becomes

$$N\,(r,\,\alpha) \;=\; f_o\,(r) + \alpha^2 f_2\,(r) + \alpha^4 f_4\,(r) + \alpha^6 f_6\,(r) + \ldots, \qquad (7)$$

where

$$f_o\,(r) \;=\; N\,(r,\,0) \qquad (8)$$

$$f_2\,(r) \;=\; \frac{k\,r}{2}\,f_o\left[F + \frac{1}{k\,H_2} - 1\right] \qquad (9)$$

$$f_4\,(r) \;=\; \tfrac{1}{2}\left(\frac{k\,r}{2}\right)^2 f_o\left[F^2 + 2\left(\frac{1}{k\,H_2} - 2\right)F + \left(\frac{1}{k\,H_2} - 1\right)^2\right] \qquad (10)$$

$$f_6\,(r) \;=\; \frac{1}{6}\left(\frac{k\,r}{2}\right)^3 f_o\left[F^3 + 3\left(\frac{1}{k\,H_2} - 3\right)F^2 + \left(\frac{3}{k^2\,H_2^2} - \frac{12}{k\,H_2} + 13\right)F + \left(\frac{1}{k\,H_2} - 1\right)^3\right]. \qquad (11)$$

Since these coefficients are the same as those given in GS (equations (38), (43), (52) and (53)), the solution is substantially the same as the one obtained there, and may be shown to be the solution for zero diffusion velocity.

Features of the Solution

The variation with latitude, α, of N at fixed height is clearly determined by the function

$$G \;=\; \exp - \tfrac{1}{2}\left[\left(k - \frac{1}{H_2}\right) r \sec^2\alpha + e^{k(r_{mo} - r\sec^2\alpha)}\right] \qquad (12)$$

This is a function of only the line of force parameter $r_o = r \sec^2 \alpha$. The maximum value of N with respect to α occurs on the line of force

$$r_o = r_{mo} - k^{-1} \log \left(1 - \frac{1}{k\, H_2}\right) \tag{13}$$

provided that

$$k\, H_2 > 1 \tag{14}$$

If $k\, H_2 \leq 1$ there is no maximum value of N with respect to α and the "trough" extends to the poles.

The height of N_{max} for constant α is r_m, where

$$r_m = \left[r_{mo} - k^{-1} \log \left(1 - \frac{\sin^2 \alpha}{k\, H_2}\right)\right] \cos^2 \alpha \quad . \tag{15}$$

Note that N_{max} is at infinite height for latitudes such that $\sin^2 \alpha > k\, H_2$. The value of N_{max} is given by

$$N_{max} = N\,(r_{mo}, 0) \left(1 - \frac{\sin^2 \alpha}{k\, H_2}\right)^{\frac{1}{2}\left(1 - \frac{\sin^2 \alpha}{k\, H_2}\right)} \exp \left(\frac{r_m \sin^2 \alpha}{2\, H_2}\right) \quad . \tag{16}$$

Comparing with the function $(1 - x)^{\frac{1}{2}(1-x)} \exp \frac{1}{2} \lambda x$, which has a turning point at $x = 1 - \exp (\lambda - 1)$, it is found that, since $\lambda = 68.5$, N_{max} has no real turning points. It follows that N_{max} has no maximum with respect to α. The value of N_{max} increases monotonically towards the poles and the "trough" in N_{max} extends to the poles. The physical explanation of this is that the ionization along a particular line of force increases away from the equator according to the diffusive equilibrium law exp $(-z/2H_2)$. N_{max} therefore lies on or near the line of force $r_o = r_{mo}$ and increases away from the equator.

The results obtained may be summarized as follows. If $k\ H_2 > 1$ there is an angular maximum of N at fixed height (i.e. an equatorial trough in N). If $k\ H_2 \leq 1$ there is no angular maximum of N at fixed height (i.e. the trough in N extends as far as the poles). In the latter case, N_{max} is at infinity for latitudes such that $\sin^2 \alpha > k\ H_2$. In all cases the trough in N_{max} extends to the poles.

General Discussion of Results

The solution represented by equation (5) thus predicts an equatorial trough of electron density at fixed height, but does not reproduce a maximum of N with respect to latitude unless $k\ H_2 > 1$. This is illustrated by figures 1 - 7, which have been computed for values of r_{mo}, k, and N_m roughly representative of high, intermediate, and low sunspot number (See Table 1), taking 6370 km as the mean radius of the earth.

[Insert Table 1 here]

It is clear that $k\ H_2$ is the most important parameter in the problem. On general grounds, this is expected to be close to unity, but the theory has neglected a number of factors, such as variations of the scale heights with altitude, which are known to occur due to the change of ionic composition. It follows that small departures from the condition $k H_2 = 1$ are not unreasonable for a simplified theory.

Since electron production, loss and diffusion are thought to become comparable near the F2 electron peak, the assumptions made in the theory are not well maintained for N_{max} over large ranges of the variable α.

Figure 4 of GS incorrectly shows a flattening of the variation of h_m with increasing α. Computed values of h_m and N_m are shown in figure 8 for values of the parameters corresponding to figure 3.

The curves for other cases are substantially similar. The series expansion approach indicates that the solution represents a continuation formula, whose terms, beyond the first, much be developed with increasing accuracy of larger α to maintain a constant accuracy in N. The approximations made in the theory result in errors which increase with α so that increasing discrepancies with the observations are to be expected for increasing α.

Comparison With Observed Data Above the F2 Electron Peak

We are indebted to Dr. J. W. King, of the Radio Research Station, Slough, England, for data supplied from the Alouette (S-27) Satellite taken on 3 October 1962 at approximately 10.20 L.M.T. over Singapore. These, together with curves computed from equation (5), are shown in figure 9. The major features of the observations are quite well reproduced with $k H_2 = 1.04 \pm 0.02$, even though the equatorial distribution was not very well represented by a Chapman profile. In particular it is to be noted that the maximum values of N with respect to latitude are seen to fall on a magnetic field line, as predicted by equation (13).

The Vertical Slope at High Altitudes

The vertical slope, $\partial (\log N)/\partial r$, is frequently used as a measure of inverse scale height, from which deductions are made concerning the temperature and mean molecular mass. It is, consequently, pertinent to inquire how this is expected to change with α on the present theory.

At high altitudes, equation (5) gives

$$\frac{\partial}{\partial r} (\log N) = -\tfrac{1}{2} m \tag{17}$$

where

$$m = k \left[1 + \left(1 - \frac{1}{k H_2} \right) \tan^2 \alpha \right] . \tag{18}$$

Thus, $m = k$ at $\alpha = 0$, and the variation of m with α is given by equation (18). This is illustrated in figure 10, where curves A, B, and C correspond to the parameters of figures 1 to 3, respectively, and curve D corresponds to the fit obtained with the satellite data in figure 8, with $k H_2 = 1.04$.

It is seen that only a very small variation is expected at moderate latitudes.

Conclusion

Figures 1 to 7 illustrate broadly one of the more interesting features of the results obtained. An angular maximum appears in the electron density N at fixed height only if $k H_2 > 1$. If the topside of the F2 layer were in a state of diffusive equilibrium, and if a Chapman function were a good approximation to the equatorial height profile, this would yield an immediate criterion for the formation of an angular maximum in N and enable the value of $k H_2$ to be determined by a curve-matching procedure. Comparison of theoretical curves with experimental data from the Alouette satellite is favorable. (See figure 9). Allowing for the crudeness of the present theory, the similarity between the theoretical and experimental curves is strong.

At present the theory does not yield an angular maximum in N_{max}. In view of the present work, and the calculations of Kendall [1963] and of Rishbeth et al. [1963],[4] it is clear that to produce an angular

[4]The differences between their work and the work of Goldberg and Schmerling discussed here (GS) were mentioned briefly by Rishbeth et al. in a note added in proof. Unfortunately the editing of their note has altered its meaning.

maximum in N_{max} requires the inclusion of effects neglected here, which might be the incorporation of production and loss or the transport of electrons by electrodynamic means. These more complicated calculations do not, however, preclude the discovery of a simplified model which might take account of a complicated process in a simple way.

The conclusions of the present paper must be regarded as replacing those in GS. It is now believed that the work applies, strictly, only to the upper parts of the F2 layer above the peak.

References

Chapman, S., The absorption and dissociative or ionizing effect of monochromatic radiation in an atmosphere on a rotating earth, _Proc. Phys. Soc._, _43_, 26, 1931.

Goldberg, R. A. and E. R. Schmerling, The distribution of electrons near the magnetic equator, _J. Geophys. Res._, _62_, 3813-3815, 1962.

Goldberg, R. A. and E. R. Schmerling, The effect of diffusion on the equilibrium electron density distribution in the F region near the magnetic equator, _J. Geophys. Res._, _68_, 1927-1936, 1963.

Kendall, P. C., Geomagnetic control of diffusion in the F2 region of the ionosphere - I The form of the diffusion operator, _J. Atmos. Terr. Phys._, _24_, 805-811, 1962.

Kendall, P. C., Geomagnetic control of diffusion in the F2 region of the ionosphere - II Numerical results, _J. Atmos. Terr. Phys._, _25_, 87-91, 1963.

Ratcliffe, J. A., E. R. Schmerling, C. S. Setty and J. O. Thomas, The rates of production and loss of electrons in the F region of the ionosphere, _Phil. Trans._, _A_ _248_, 621-642, 1956.

Rishbeth, H., A. J. Lyon and M. Peart, Diffusion in the equatorial F layer, _J. Geophys. Res._, _68_, 2559-2569, 1963.

Legends for Diagrams

Figure 1 - Computed curves of electron density versus dip angle for high sunspot number. (See Table 1)

Figure 2 - Computed curves of electron density versus dip angle for high sunspot number. (See Table 1)

Figure 3 - Computed curves of electron density versus dip angle for high sunspot number. (See Table 1)

Figure 4 - Computed curves of electron density versus dip angle for intermediate sunspot number. (See Table 1)

Figure 5 - Computed curves of electron density versus dip angle for intermediate sunspot number. (See Table 1)

Figure 6 - Computed curves of electron density versus dip angle for low sunspot number. (See Table 1)

Figure 7 - Computed curves of electron density versus dip angle for low sunspot number. (See Table 1)

Figure 8 - Top: Variation of the height of peak electron density, h_mF2, with dip angle.

Bottom: Variation of the peak electron density, N_mF2, with dip angle.

Figure 9 - Comparison of theoretical curves with Alouette observations.

Figure 10 - Variation of $[\partial (\log N)/\partial r]^{-1}$ (the measure of "scale height") with dip angle.

Table 1 - Numerical Parameters used in the computation of Figures 1 through 7.

TABLE 1

	r_{mo} (km)	N_m ($x\ 10^{-5}$ electrons/cc)	H_2 (km)	k (km^{-1})	kH_2	
fig 1	6850	19.25	75	.01	.75	High sunspot number
fig 2	6850	19.25	100	.01	1.00	
fig 3	6850	19.25	112.5	.01	1.125	
fig 4	6800	10.00	75	.0133	1.00	Intermediate sunspot number
fig 5	6800	10.00	85	.0133	1.13	
fig 6	6750	6.00	50	.02	1.00	low sunspot number
fig 7	6750	6.00	57	.02	1.14	

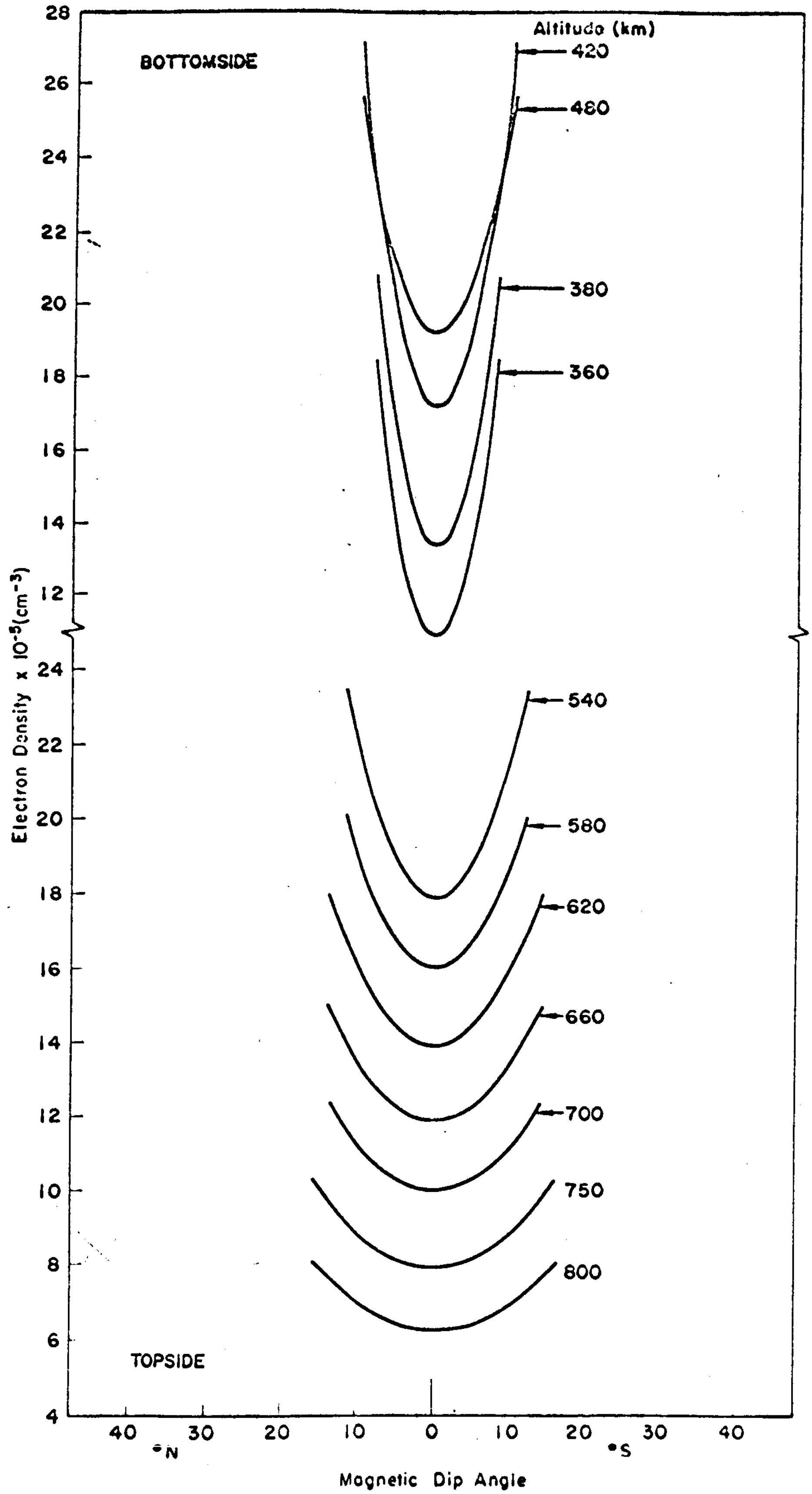

BOTTOMSIDE
Altitude (km)
420
480
380
360
540
580
620
660
700
750
800
TOPSIDE
Electron Density x 10⁻⁵(cm⁻³)
28
26
24
22
20
18
16
14
12
24
22
20
18
16
14
12
10
8
6
4
40
30
20
10
0
10
20
30
40
°N
°S
Magnetic Dip Angle

FIG 1

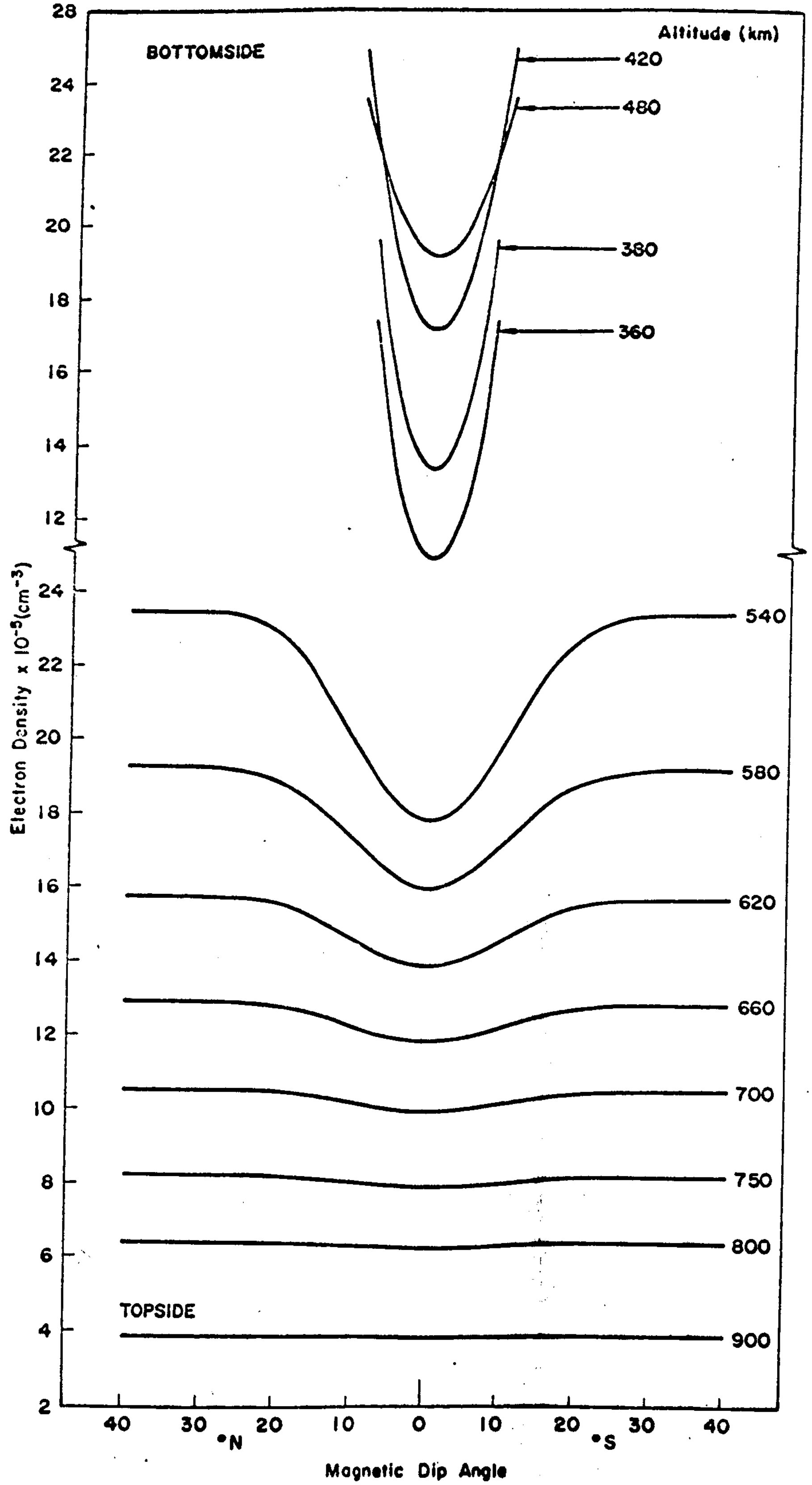
BOTTOMSIDE
Altitude (km)
420
480
380
360
540
580
620
660
700
750
800
900
TOPSIDE
Electron Density x 10^{-5} (cm^{-3})
28
24
22
20
18
16
14
12
10
8
6
4
2
40
30
20
10
0
°N
°S
Magnetic Dip Angle

FIG 2

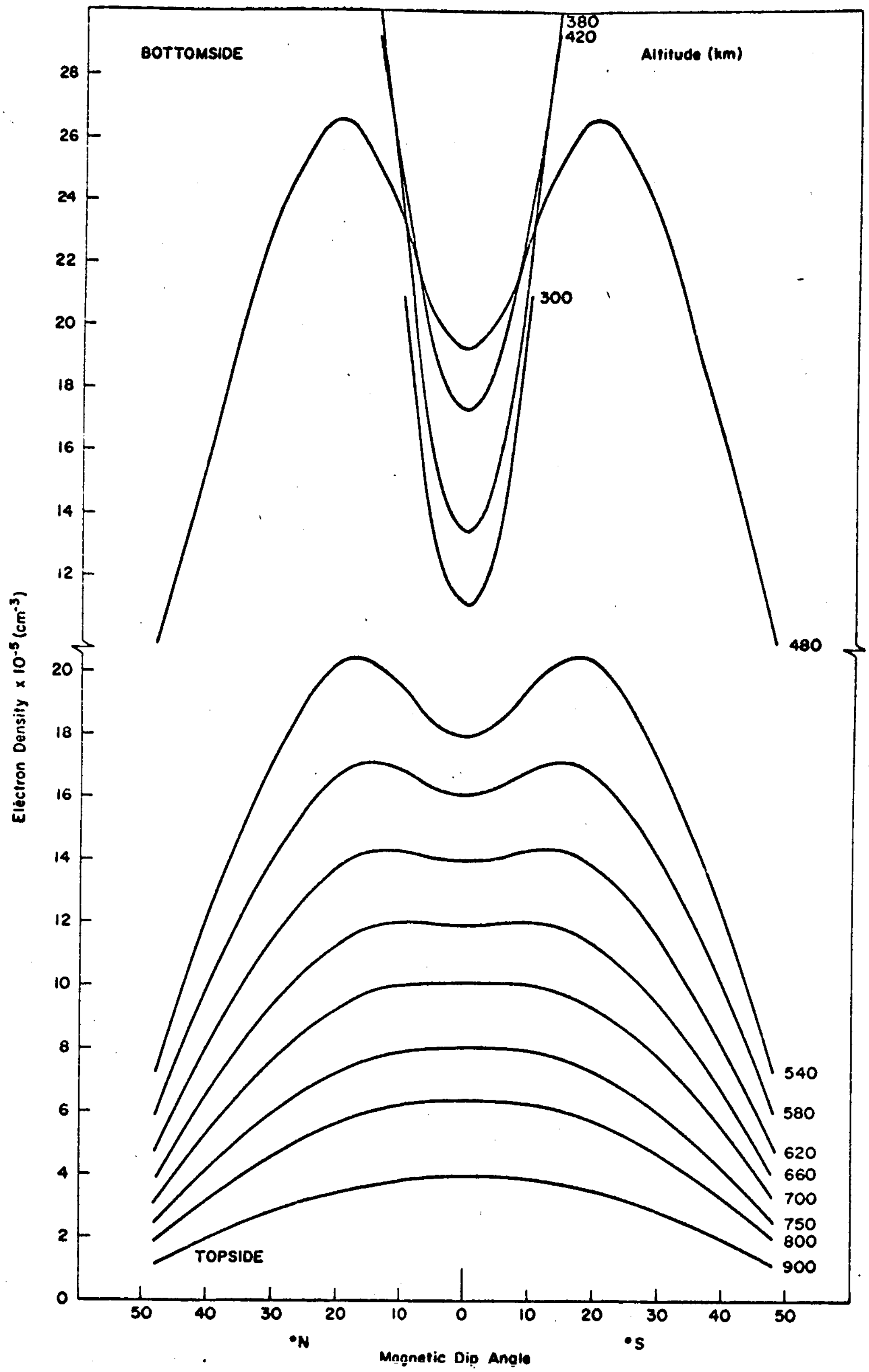
BOTTOMSIDE
Altitude (km)
380
420
300
480
540
580
620
660
700
750
800
900
TOPSIDE
Electron Density x 10^{-5} (cm^{-3})
°N
°S
Magnetic Dip Angle

FIG 3

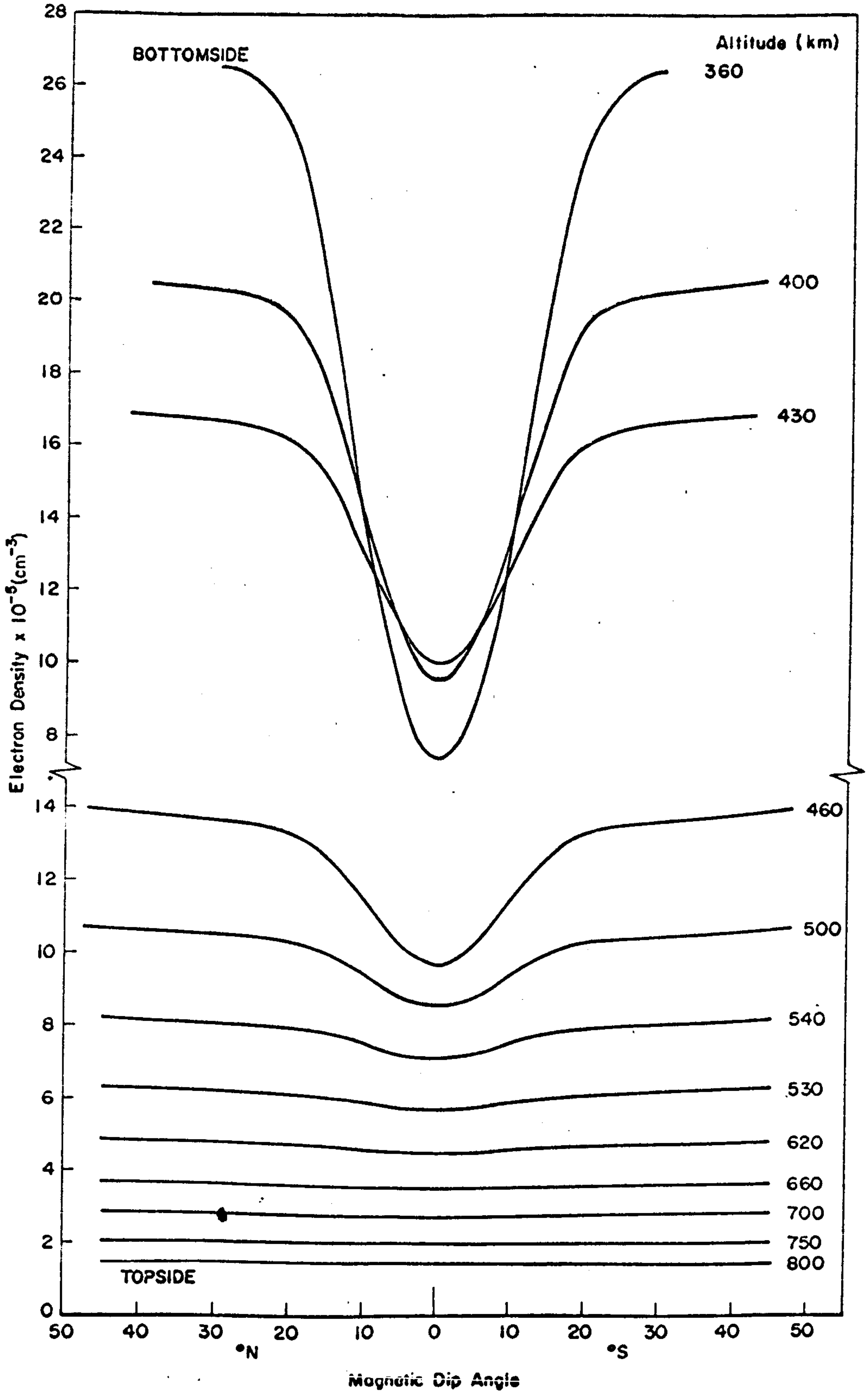
BOTTOMSIDE
Altitude (km)
360
400
430
460
500
540
530
620
660
700
750
800
TOPSIDE
Electron Density x 10^{-5}(cm^{-3})
28
26
24
22
20
18
16
14
12
10
8
14
12
10
8
6
4
2
0
50
40
30
20
10
0
10
20
30
40
50
°N
°S
Magnetic Dip Angle

FIG 4

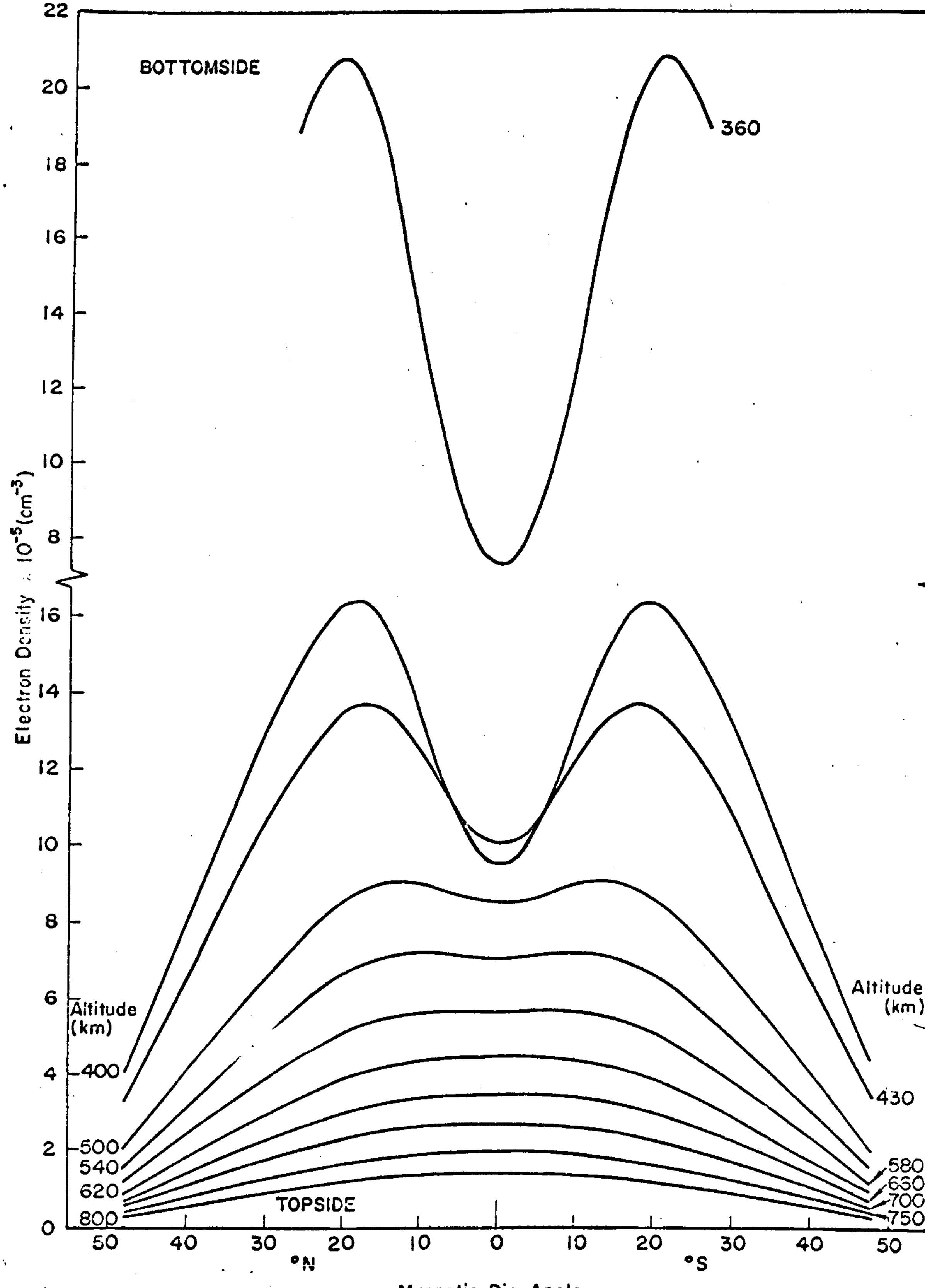

BOTTOMSIDE
360
Electron Density × 10^-5 (cm^-3)
Altitude (km)
400
500
540
620
800
TOPSIDE
Altitude (km)
430
580
660
700
750
°N
°S
Magnetic Dip Angle

F165

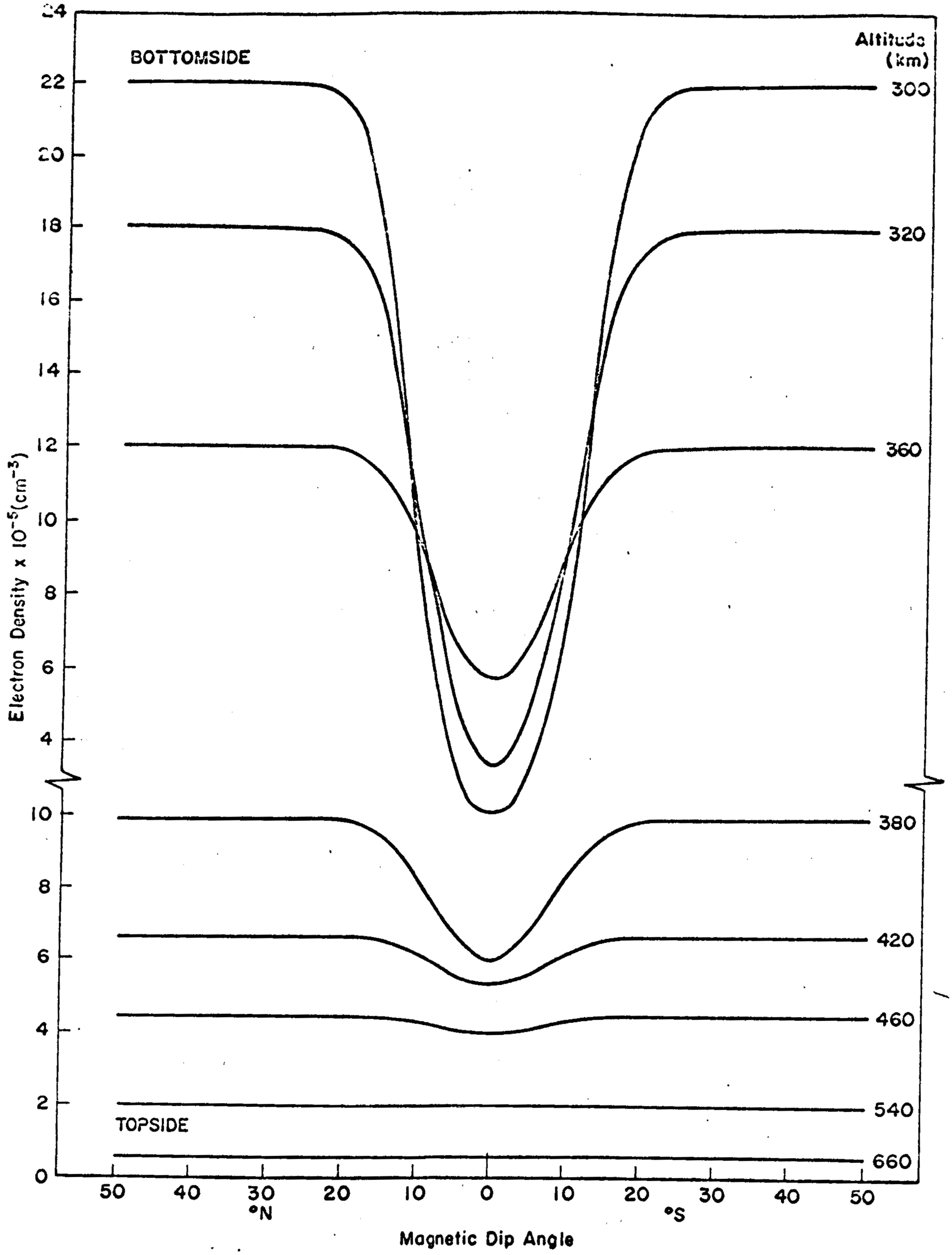
BOTTOMSIDE
TOPSIDE
Altitude (km)
300
320
360
380
420
460
540
660
Electron Density x 10^{-5} (cm^{-3})
24
22
20
18
16
14
12
10
8
6
4
10
8
6
4
2
0
50
40
30
20
10
0
10
20
30
40
50
°N
°S
Magnetic Dip Angle

FIG 6

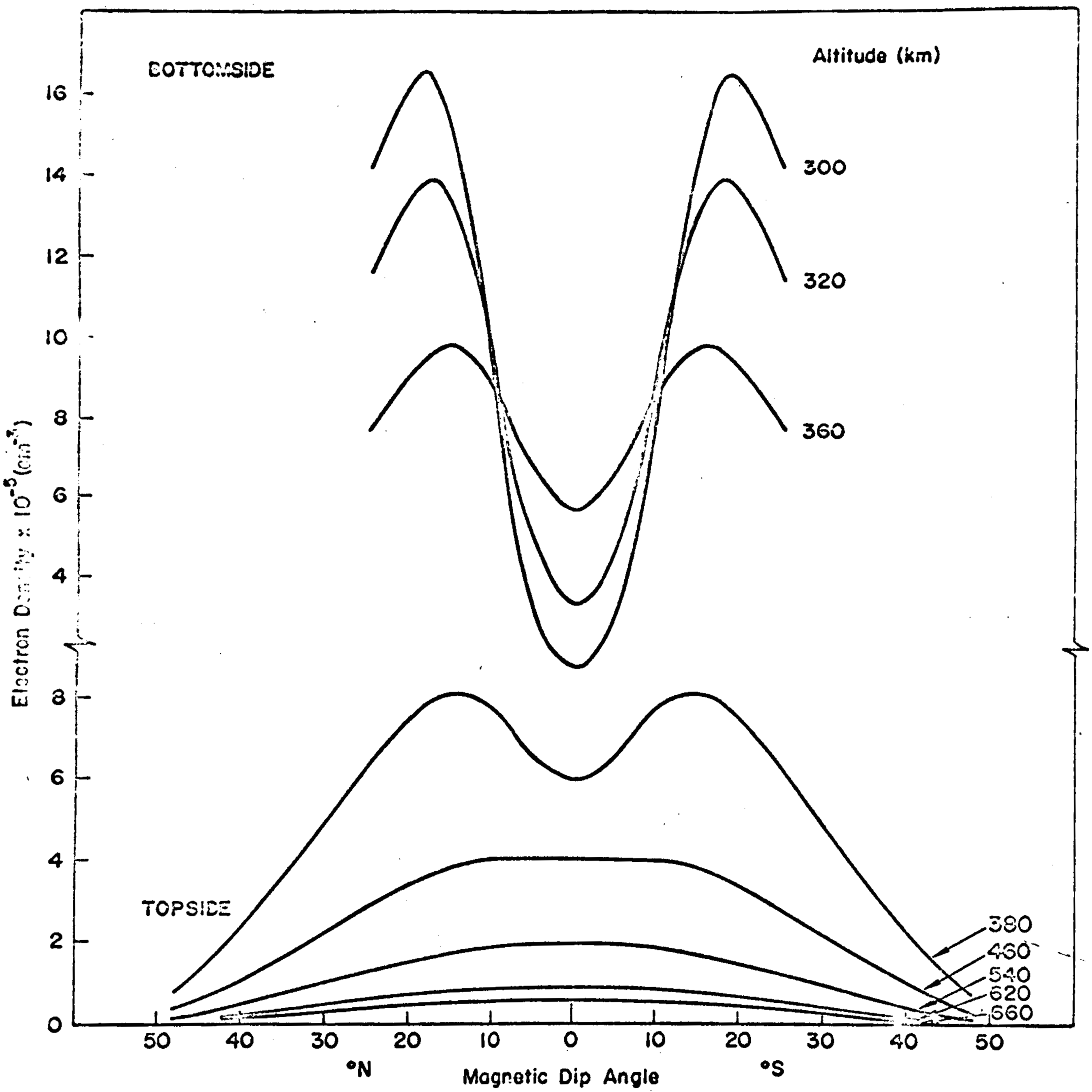

BOTTOMSIDE
Altitude (km)
300
320
360
TOPSIDE
380
460
540
620
660
Electron Density × 10^-5 (cm^-3)
°N
Magnetic Dip Angle
°S

FIG 7

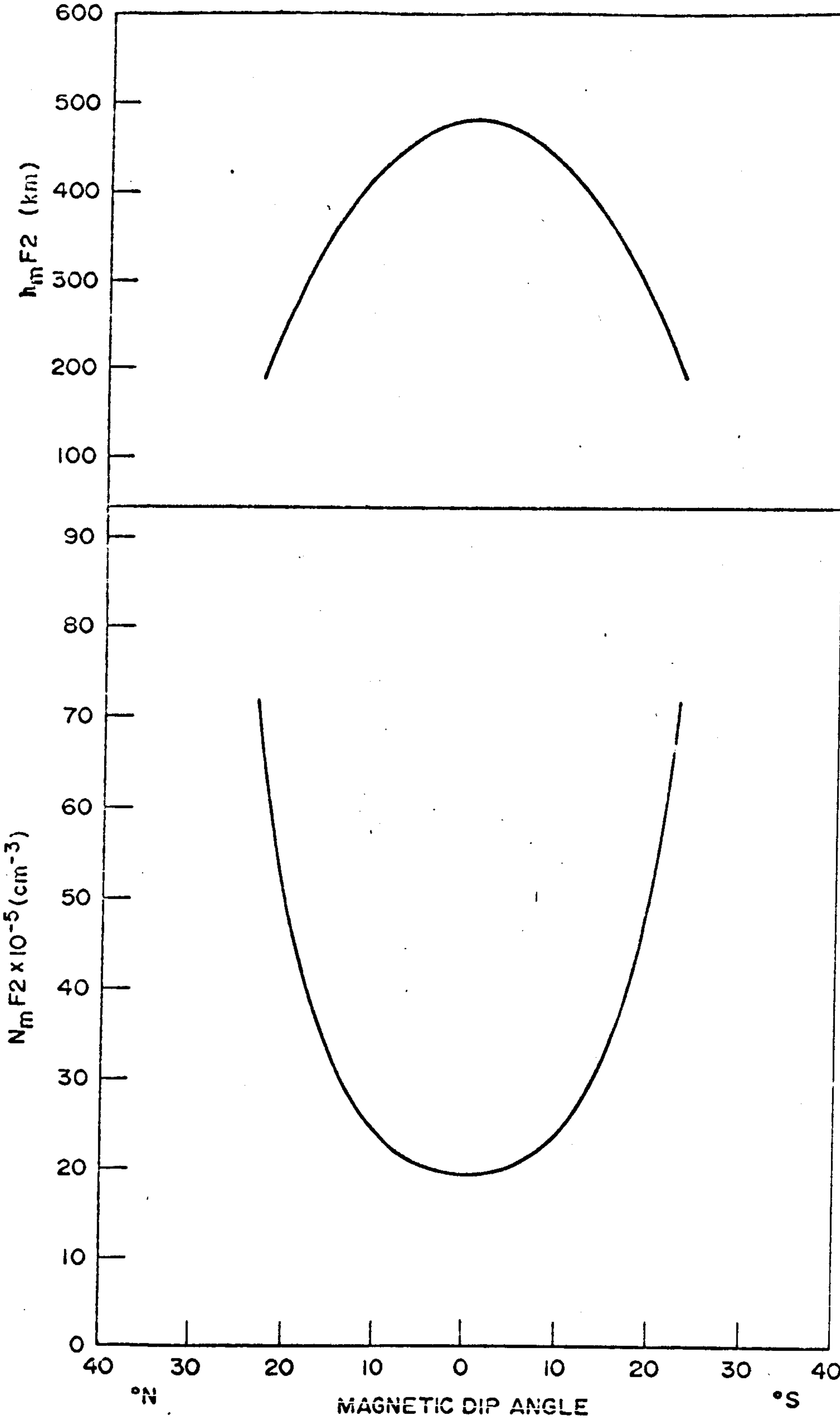

600
500
400
300
200
100
h_mF2 (km)
90
80
70
60
50
40
30
20
10
0
$N_mF2 \times 10^{-5} (cm^{-3})$
40
30
20
10
0
10
20
30
40
°N
MAGNETIC DIP ANGLE
°S

FIG 8

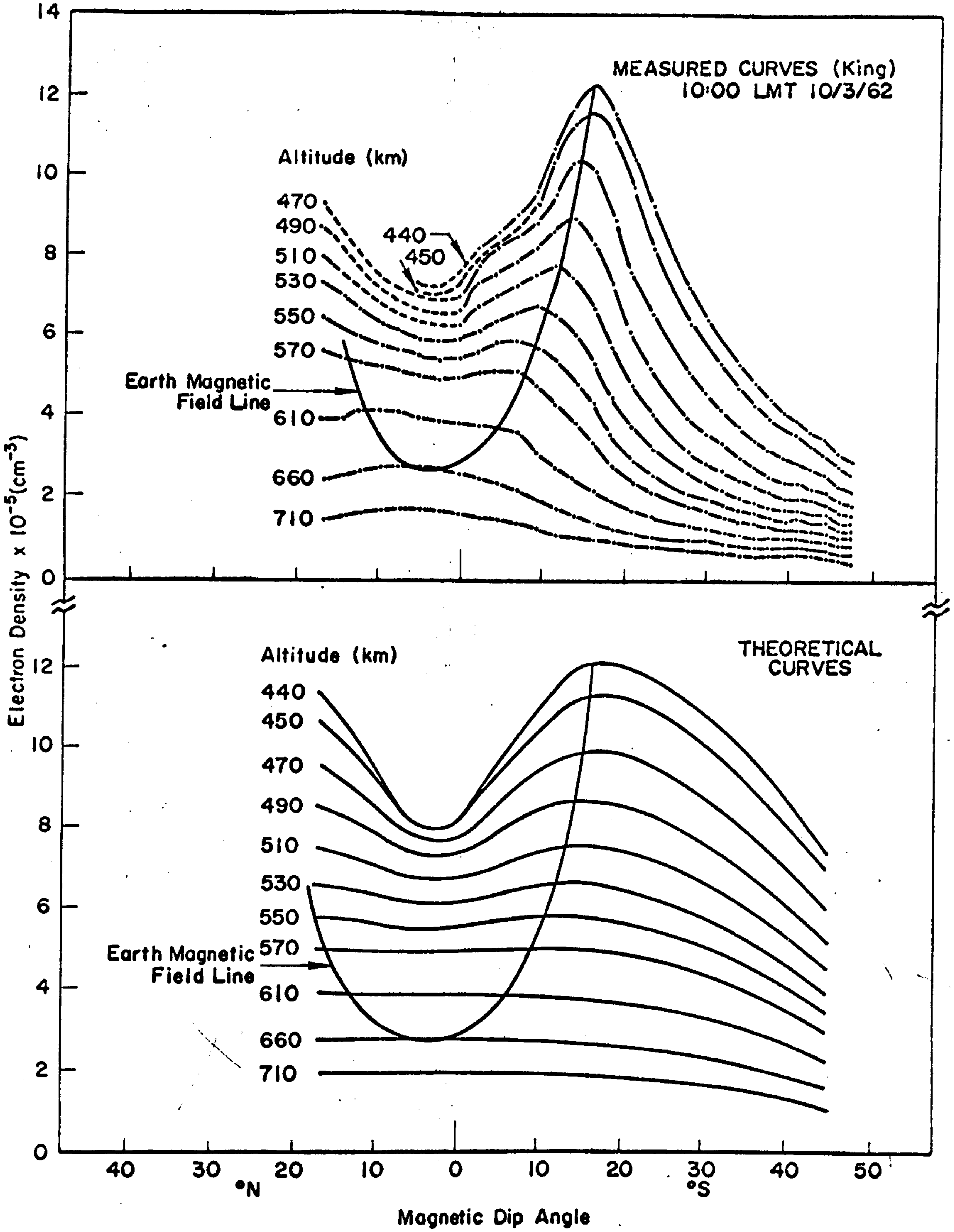

MEASURED CURVES (King)
10:00 LMT 10/3/62
Altitude (km)
470
490
510
530
550
570
610
660
710
440
450
Earth Magnetic Field Line
THEORETICAL CURVES
Altitude (km)
440
450
470
490
510
530
550
570
610
660
710
Earth Magnetic Field Line
Electron Density x 10^{-5}(cm^{-3})
0
2
4
6
8
10
12
14
40
30
20
10
0
10
20
30
40
50
°N
°S
Magnetic Dip Angle

FIG 9

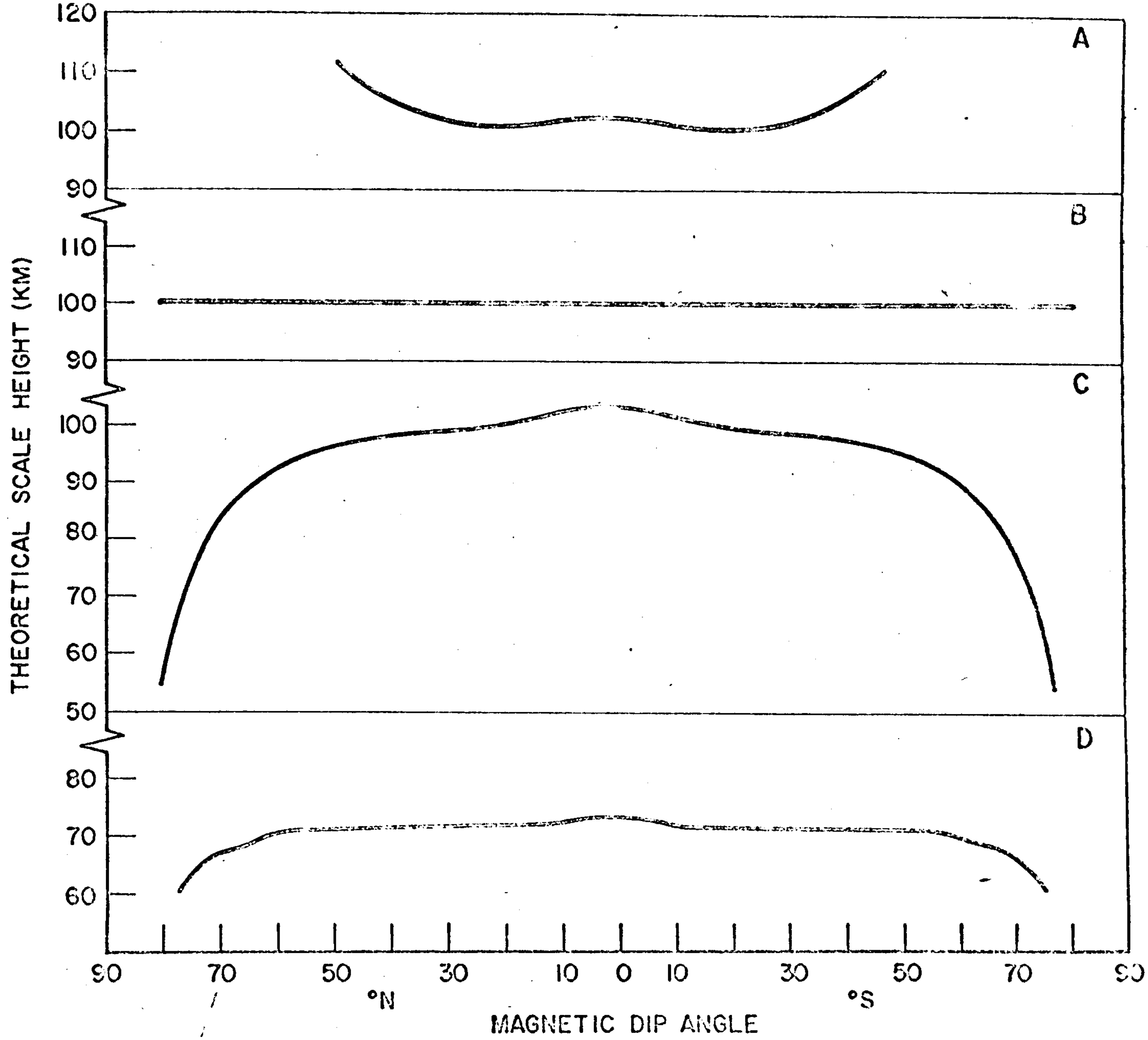
A
B
C
D
120
110
100
90
80
70
60
50
THEORETICAL SCALE HEIGHT (KM)
90
70
50
30
10
0
°N
°S
MAGNETIC DIP ANGLE

FIG 10